Soil Dynamics and Earthquake Engineering 85 (2016) 179–190

Contents lists available at ScienceDirect

Soil Dynamics and Earthquake Engineering

journal homepage: www.elsevier.com/locate/soildyn

On the seismic stability and critical slip surface of reinforced slopes

M. Khosravizadeh [a], M. Dehestani [b,*], F. Kalantary [c]

[a] Department of Civil Engineering, University of Guilan, Rasht, Iran
[b] Faculty of Civil Engineering, Babol Noshirvani University of Technology, Babol, Iran
[c] Faculty of Civil Engineering, K.N. Toosi University of Technology, Tehran, Iran

ARTICLE INFO

Article history:
Received 8 June 2015
Received in revised form
28 March 2016
Accepted 29 March 2016

Keywords:
Horizontal Slice Method
Seismic stability
Pseudo-static force
Reinforced slope
Multiplanar slip surface

ABSTRACT

Seismic stability of reinforced slopes is investigated using Horizontal Slice Method within the framework of the pseudo-static force. These introduced by constant horizontal or vertical inertial forces and the equilibrium equations for all forces applied to each horizontal slice are considered. A new procedure is introduced which could determine the location and shape of failure surface. The slip surface is a multiplanar surface consisting of a number of inclined linear segments interconnected with various lengths and angles in a plane. The amount of reinforcement forces is used as the objective function in the optimization procedure to determine the shape and location of the critical slip surface. This approach is relatively simple and yields results which are in good agreement with previous findings. Final results revealed that with increase in horizontal seismic acceleration, the reinforcements force increases. With increase in slope angle, the failure surface changes from curve to planar shape.

1. Introduction

Stability analysis of natural and artificial slopes is an interesting issue in civil, geotechnical and mining engineering. In addition, the design and safety evaluation of reinforced structures subject to seismic loading is an important problem (Richardson and Lee [1], Bathurst and Cai [2], Jones and Clarke [3]).

In recent decades, a technique based on limit state approach has been employed in several studies (Ling et al. [4], Ling and Leshchinsky [5], Michalowski [6], Ausilio et al. [7]) to evaluate the seismic stability of slopes. Ling et al. [4] utilized the pseudo-static limit equilibrium approach for the seismic analysis of reinforced soil structures subject to seismic horizontal acceleration. Subsequently, Ling and Leshchinsky [5] extended their studies and examined the effect of vertical earthquake acceleration. Michalowski [6] and Ausilio et al. [7] used the kinematic approach of limit analysis to analyze the seismic stability of retaining structures.

Horizontal Slice Method (HSM) is a new analytical method based on limit equilibrium proposed by Lo and Xu [8]. This method has been used later by Shahgholi et al. [9] and Nouri et al. [10]. In this method, the sliding block is divided into several finite horizontal rigid slices parallel to reinforcements and then the equilibrium equations are considered for each slice. Effects of seismic loads are taken into account as pseudo-static forces. The crucial point in using HSM for stability analysis is how to find out the location and configuration of the slip surface. Different trial slip surface have been used by various researchers include planar (e.g., Saran et al. [11]; Narasimha Reddy et al. [12]), circular (e.g., Sengupta and Upadhyay [13]; Kalatehjari et al. [14]), non-circular (e.g., Zolfaghari et al. [15]; Nimbalkar et al. [16]).

For coarse-grained soil and also steep slopes, the slip surface is approximately planar [17]. Circular failure surface is used for cohesive and homogeneous soil slopes [18], and non-circular failure surfaces are occurred in non-homogeneous slope (e.g., Morgenstern and Price [19], Spencer [20]). Non-circular failure surface can be formed from arcs of a circle or log-spiral together with linear segments or just with straight line segments [21]. Prater [22] assumed sliding surface of circular and logarithmic spiral types and investigated the stability conditions for homogeneous soils. Although the different failure states are reported in the literatures, the real failure surface shape has not been obtained yet. For real cases, the location of slip surface is often unknown and sliding of a slope is not smooth and sometimes takes arbitrary shapes. In most of the studies, the shape of the slip surface is predefined. However, the configuration of the slip surface is affected by geotechnical and geometric characteristics of slopes [23]. There are various methods for obtaining the critical slip surface. Hu et al. [24] determined the noncircular slip surface using mutative scale chaos optimization algorithm. Nguyen [25] used the simplex reflection method to find critical slip surfaces. Malkawi et al. [26] adopted the Monte Carlo optimization procedure to identify the critical slip surfaces. Also, a number of researchers have used genetic algorithm to search for the slip surface (Goh [27]; Zolfaghari et al. [15]).

* Corresponding author. Tel.: +98 9113136113; fax: +98 1132331707.
E-mail addresses: mkhosravizadeh@gmail.com (M. Khosravizadeh), dehestani@nit.ac.ir (M. Dehestani), fz_kalantary@kntu.ac.ir (F. Kalantary).

http://dx.doi.org/10.1016/j.soildyn.2016.03.018
0267-7261/

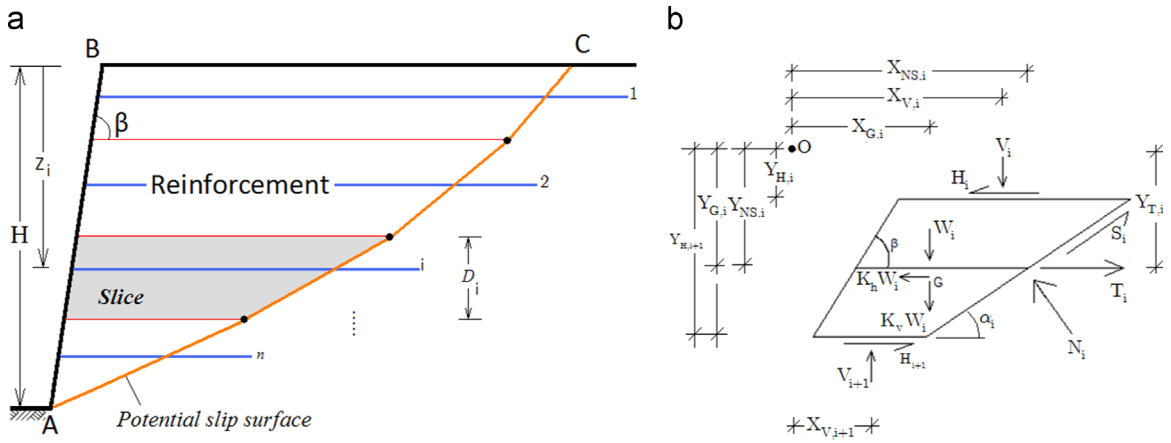

Fig. 1. (a) General slope configuration and (b) acting forces on each slice.

Sarma and Tan [28] used a new method to determine the critical slip surface based on the limit equilibrium technique with added stress acceptability criterion, for both homogeneous and non-homogeneous slopes. No prior assumption of the shape of the surface is needed. In this method, the slip surface, which comprises a series of straight lines, was obtained slice by slice going uphill. The slip surface and the interslice boundaries were not predefined. But, the effect of reinforcement elements on stability was not considered. Then, Stamatopoulos et al. [29] extended the method proposed by Sarma [30] to dynamic problems using a developed multiblock model.

Therefore, determination of the critical slip surface is one of the key problems in slope stability evaluation.

In this study, Horizontal Slice Method is employed to analyze slope stability and also to achieve the position and configuration of the critical slip surface in slopes. The procedure yields a new multiplanar shape as an accurate approximation for the shape of the failure surface. Location of failure surface can be determined eventually.

2. Method of analysis

2.1. Horizontal Slice Method

In the comprehensive formulation proposed by Nouri et al. [10], the equilibrium of all vertical and horizontal forces and also the moment equilibrium in each slice of the logarithmic spiral slip surface are satisfied. They have called this formulation as rigorous formulation also known as $(5n-1)$ formulation. In this study a similar formulation, within the framework of the limit equilibrium technique of HSM is considered for homogeneous reinforced slopes.

The main difference between the present method and those of previous studies is that no prior configuration is assumed for slip surface. In order to obtain the equilibrium equations, consider a slope with general shape shown in Fig. 1.

T_i is the tension force in the i-th reinforcement layer. N_i and S_i are respectively the normal and shear forces acting on the base of each slice. W_i is the weight of the i-th slice, and α_i is the inclination angle of the slice base. k_h and k_v are the horizontal and vertical seismic coefficients for pseudo-static analysis, respectively. H_i and V_i are the shear and normal inter-slice forces acting on each slice, respectively. V_i denotes the vertical inter-slice force which is equal to the weight of upper soil layers.

For the interface forces, two approaches exist in the bibliography: (a) the first assumes that they have fixed inclination and that is defined through a scalar coefficient, and (b) the second

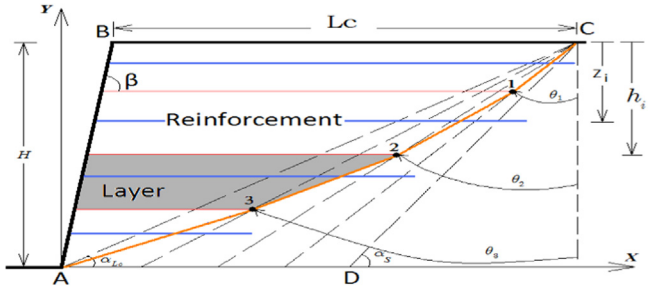

Fig. 2. The geometry of multiplanar sliding mechanism.

obtains the interface inclinations by minimizing the factor of safety. For non-circular slip surfaces, Morgenstern and Price [19] proposed the following relationship:

$$H_i = \lambda V_i \tag{1}$$

where λ is a coefficient ranging between 0 and 1.

In the method provided by Sarma [30], the shear strength was mobilized on the interslice boundaries and the inclination of slice interfaces is varied to produce a critical condition. The method provided by Sarma uses a shear strength equation. In addition, Sarma and Tan [28] have implicitly assumed that the Mohr–Coulomb criterion is satisfied along the vertical interfaces between slices. Nouri et al. [10] obtained the interslice forces via a trial and error procedure in the last piece. In the proposed method, the inclination of the inter-slice forces are taken to be independent of k_h and defined as $\lambda = (1 - \beta/100)\tan(\varphi)/F.S$.

Earthquake effects can be taken into account by assuming the sliding mass subjected to both vertical and horizontal pseudo-static forces. However, the vertical force is usually ignored in the standard pseudo-static analysis. This is due to the fact that the vertical seismic force acting on the sliding mass usually has negligible effect on the stability of a slope. The moment equilibrium equations require the location of the application of the normal force on the slip surface. The usual assumption of 'middle of the slice' is a good and reasonable one [10]. Hence, the equilibrium equations of the force and moment for each slice in x-y plane are proposed the by Nouri et al. [10], following relationship

$$\sum F_x = 0 \Rightarrow T_i + S_i\cos(a_i) - N_i\sin(a_i) - k_h W_i + H_{i+1} - H_i = 0 \tag{2}$$

$$\sum F_y = 0 \Rightarrow V_{i+1} - V_i - (1 + k_v)W_i + S_i\sin(a_i) + N_i\cos(a_i) = 0 \tag{3}$$

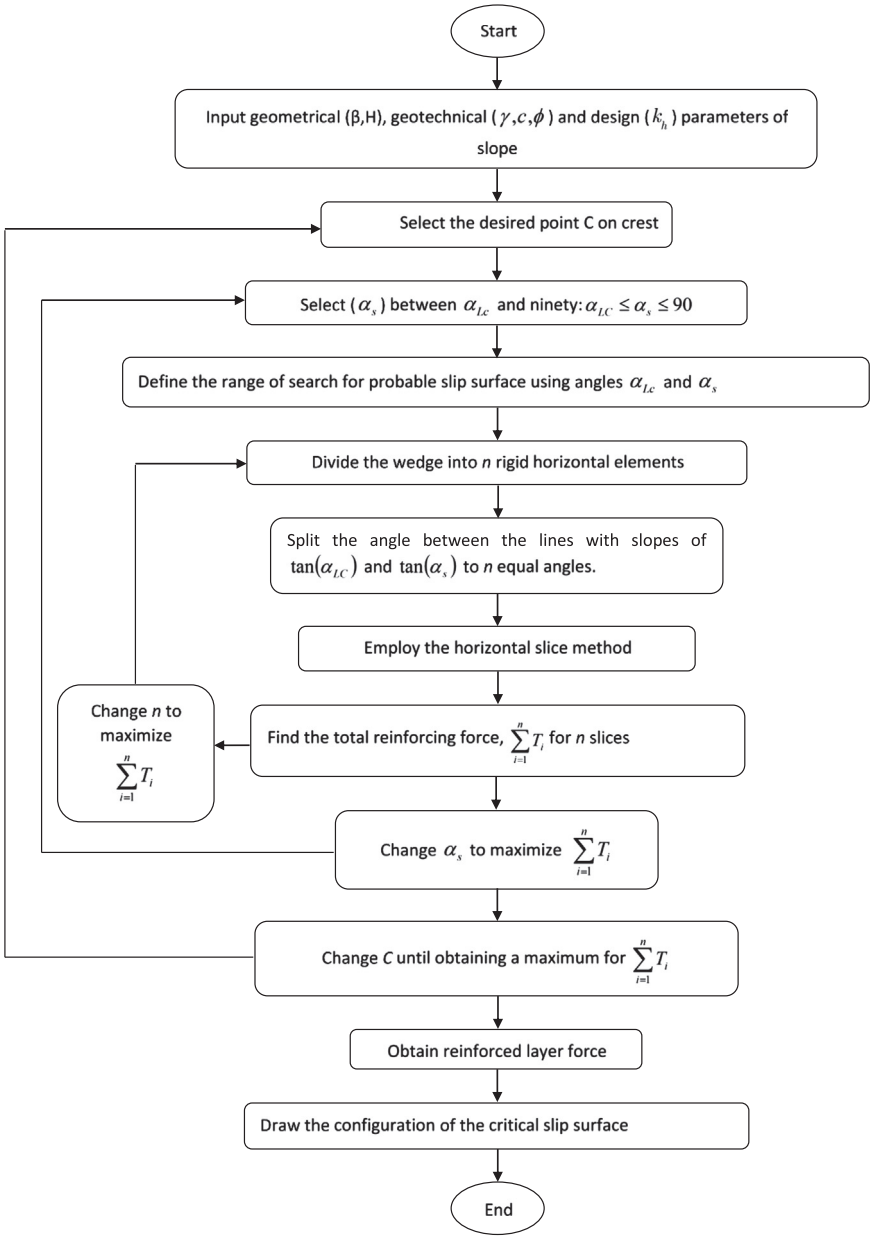

Fig. 3. Flowchart of calculations for Horizontal Slice Method.

$$\sum M_O = 0 \Rightarrow$$

$$V_{i+1}X_{V,i+1} - V_iX_{V,i} + T_iY_{T,i} + H_{i+1}Y_{H,i+1} - H_iY_{H,i} - (1 + k_v)W_iX_{G,i} - (k_hW_i)Y_{G,i} + [S_i\cos(\alpha_i) + N_i\sin(\alpha_i)]Y_{NS,i} + [S_i\sin(\alpha_i) + N_i\cos(\alpha_i)]X_{NS,i} = 0 \quad (4)$$

$Y_{NS,i}$ and $X_{NS,i}$ are the coordinates of the point where N_i and S_i act on the base of the slice with respect to the point denoted by O. X_V and Y_H are the coordinates of the point of application of vertical and horizontal interslice forces on the slice with respect to the point denoted by O. In addition, $X_{G,i}$ and $Y_{G,i}$ are the coordinates of the point of application of vertical and horizontal pseudo-static forces on the center of gravity of each slice with respect to the point denoted by O.

According to Mohr–Coulomb failure envelope, the relation between the shear and normal forces at the failure stage is expressed by

$$S_i = \frac{1}{F.S.}[Cb_i + N_i\tan(\phi)] \quad (5)$$

where C and ϕ are the soil cohesion and internal friction angle, respectively. The cohesion of the backfill material is considered to be zero. $F.S.$ is factor of safety, which is assumed to be 1 for all of the slices. The mobilized tension force in the i-th reinforcement layer, T_i, assuming that every reinforcement is placed at the centroid of each slice, can be used in a relation proposed by Ling et al. [4], as

$$T_i = K\gamma_iZ_iD_i \quad (6)$$

where K is the total normalized reinforcement force, D_i is the distance between layers i and $i+1$. Z_i is the depth of the i-th reinforcement measured from the crest. It is assumed that all

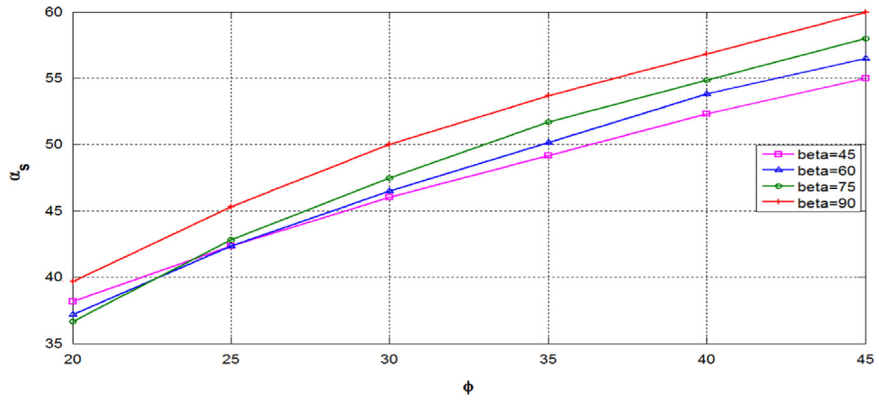

Fig. 4. Variation of α_s against ϕ for different values of β and $k_h = 0.2$.

Table 1
Various methods for finding the slip surface and their parameters.

Analysis	Method	Slip surface	Loading	Characteristics
Limit analysis	Michalowski	Log-spiral	Pseudo-static	Model slopes: homogeneous, cohesionless and free draining The kinematic theorem of limit analysis Seismic force in the horizontal direction 24 reinforced layers Safety factor is unit
	Ausilio et al.	Log-spiral	Pseudo-static	Model slopes: homogeneous, cohesionless and Free draining The kinematic theorem of limit analysis Seismic force in the horizontal direction 5,10,20 reinforced layers Safety factor is unit
Limit equilibrium	Ling et al.	Log-spiral	Pseudo-static	Model slopes: homogeneous, cohesionless and free draining Used equilibrium equation: moment for the whole wedge Horizontal Slice Method Seismic force in the horizontal direction 10 reinforced layers Safety factor is unit
	Nimbalkar et al.	Multilinear	Pseudo-dynamic	Model slopes: homogeneous, cohesionless and free draining Used equilibrium equation: forces Horizontal Slice Method Seismic force in the horizontal and vertical direction 20 reinforced layers Safety factor is unit
	Nouri et al.	Log-spiral	Pseudo-static	Model slopes: homogeneous, cohesionless and free draining Used equilibrium equation: forces and moment Horizontal Slice Method 5 reinforced layers Safety factor is unit
	Present work	Multiplanar	Pseudo-static	Model slopes: homogeneous, cohesionless and free draining Used equilibrium equation: forces and moment Horizontal Slice Method Seismic force in the horizontal direction Optimum reinforced layers Safety factor is unit

Table 2
Geometric and geotechnical characteristics of slope (Nouri et al. [31]).

Characteristics	Parameter	Values
Slope height	H	5 m
Soil cohesion	C	0
Safety factor	$F.S.$	1.00
Soil density	γ	18 kN/m^3
Coefficient of horizontal seismic acceleration	k_v	0.00
Coefficient of vertical seismic acceleration	k_h	0.00, 0.05, 0.10, 0.15, 0.20, 0.25, 0.30
Slope inclination angle	β	45° – 60° – 75° – 90°
Soil internal friction angle	ϕ	20°, 25°, 30°, 35°, 40°, 45°

reinforcements are placed at the mid-line of layers. γ_i is the unit weight of the soil.

Thus we have,

$$D_i = \frac{H}{n} \tag{7}$$

$$z_i = (i - 0.5)\frac{H}{n} \tag{8}$$

where n is the number of layers. Limit equilibrium methods determine the critical failure surface based on the minimum value of the safety factor or the maximum value of the reinforced forces. In

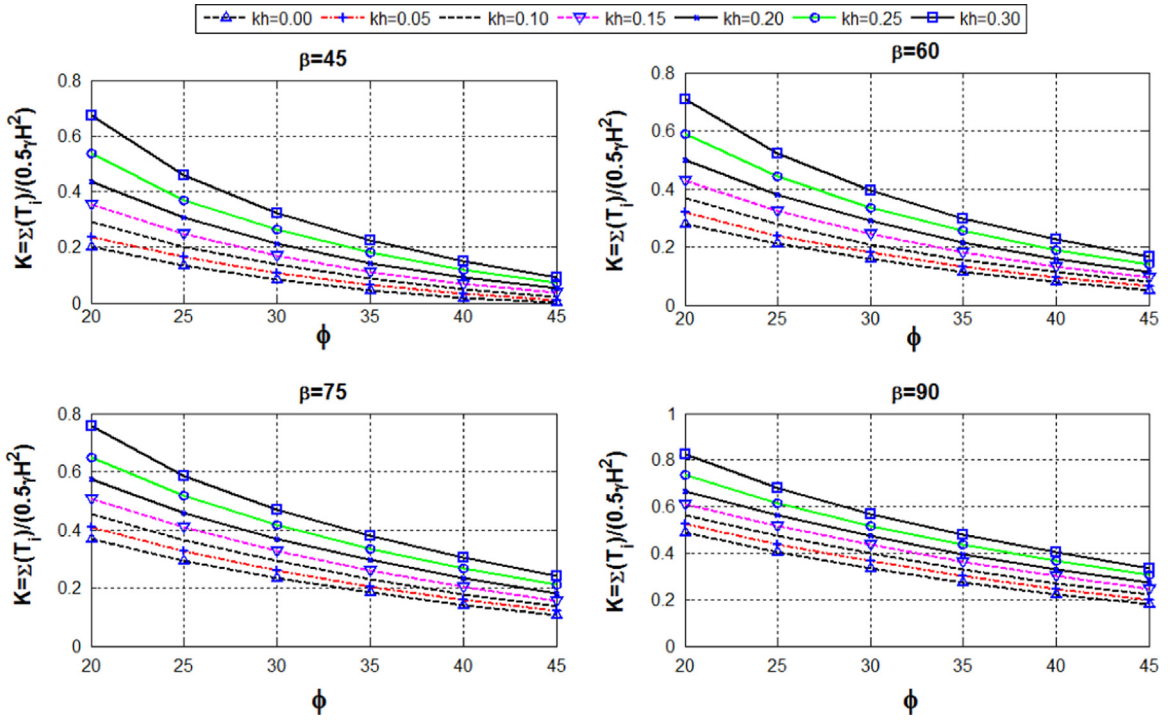

Fig. 5. Variation of K against ϕ for different values of β and k_h.

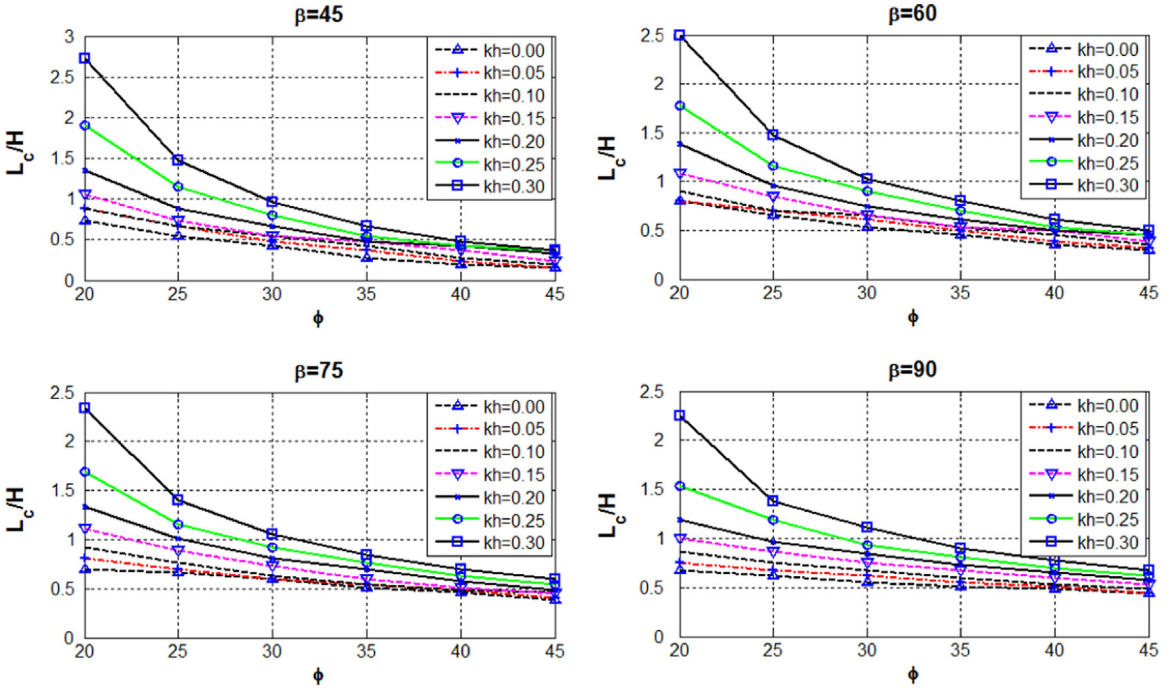

Fig. 6. Variation of L_c/H against ϕ for different values of β and k_h.

the present paper factor of safety is equal to one and thus the critical sliding surface is the surface for which the sum of the mobilized tensile force in the reinforcements become maximum. In order to have a constant value for K, the total reinforcement force was normalized as

$$K = \frac{1}{0.5(\gamma H^2)} \sum_{i=1}^{n} T_i \tag{9}$$

The base of the slope is assumed to be sufficiently hard and the critical failure surface does not pass through the foundation material. Also, the slip surface is assumed to pass through the toe of the slope in frictional soils and the effect of facing elements on stability is neglected.

2.2. Slip surface configuration

Present paper describes a new method based on equations of horizontal slices for obtaining the failure surface. It is assumed that the slip surface consists of n inclined linear segments interconnected with various lengths and angles in a plane. e.g., $n = 2$

Table 3
Results of $(\sum_{i=1}^{n} T_i)_{max}$ (kN) for a slope with $\beta = 45°$.

ϕ (deg)	$(\sum_{i=1}^{n} T_i)_{max}$ (kN)						
	k_h=0.00	k_h=0.05	k_h=0.10	k_h=0.15	k_h=0.20	k_h=0.25	k_h=0.30
20	44.00	54.00	66.00	80.00	98.00	121.00	154.00
25	29.00	36.00	45.00	56.00	69.00	84.00	103.00
30	18.00	23.00	30.00	38.00	48.00	59.00	73.00
35	10.00	14.00	19.00	25.00	32.00	41.00	51.00
40	4.00	7.00	11.00	15.00	20.00	27.00	34.00
45	0.40	2.00	5.00	8.00	12.00	16.00	22.00

Table 4
Results of $(\sum_{i=1}^{n} T_i)_{max}$ (kN) for a slope with $\beta = 60°$.

ϕ (deg)	$(\sum_{i=1}^{n} T_i)_{max}$ (kN)						
	k_h=0.00	k_h=0.05	k_h=0.10	k_h=0.15	k_h=0.20	k_h=0.25	k_h=0.30
20	62.00	72.00	83.00	96.00	112.00	133.00	161.00
25	47.00	55.00	63.00	73.00	85.00	99.00	117.00
30	35.00	41.00	48.00	56.00	65.00	76.00	88.00
35	25.00	30.00	36.00	42.00	49.00	57.00	67.00
40	16.00	20.00	26.00	31.00	37.00	43.00	51.00
45	10.00	13.00	16.00	22.00	26.00	31.00	38.00

Table 5
Results of $(\sum_{i=1}^{n} T_i)_{max}$ (kN) for a slope with $\beta = 75°$.

ϕ (deg)	$(\sum_{i=1}^{n} T_i)_{max}$ (kN)						
	k_h=0.00	k_h=0.05	k_h=0.10	k_h=0.15	k_h=0.20	k_h=0.25	k_h=0.30
20	84.00	92.00	103.00	114.00	129.00	146.00	171.00
25	67.00	74.00	83.00	93.00	104.00	116.00	132.00
30	54.00	60.00	67.00	75.00	83.00	94.00	106.00
35	42.00	48.00	54.00	60.00	67.00	76.00	85.00
40	33.00	37.00	42.00	48.00	54.00	61.00	69.00
45	25.00	29.00	33.00	38.00	43.00	49.00	55.00

Table 6
Results of $(\sum_{i=1}^{n} T_i)_{max}$ (kN) for a slope with $\beta = 90°$.

ϕ (deg)	$(\sum_{i=1}^{n} T_i)_{max}$ (kN)						
	k_h=0.00	k_h=0.05	k_h=0.10	k_h=0.15	k_h=0.20	k_h=0.25	k_h=0.30
20	111.00	119.00	128.00	139.00	151.00	167.00	187.00
25	92.00	99.00	108.00	117.00	127.00	139.00	153.00
30	76.00	82.00	90.00	98.00	107.00	117.00	128.00
35	62.00	68.00	74.00	82.00	90.00	98.00	108.00
40	50.00	55.00	61.00	68.00	75.00	82.00	91.00
45	40.00	45.00	50.00	56.00	62.00	68.00	76.00

denotes a bilinear slip surface. With increase in number of layers, the failure surface approaches to a nonlinear curve to demonstrate features of the real failure surface.

The mechanism of segmentation is illustrated in Fig. 2. For $n=4$, the angle ∠ACD is divided to 4 equal parts and segments are connected at points denoted by 1, 2, and 3. The two particular angles, α_{Lc} and α_s are inclined angles relative to the ground surface as shown in Fig. 2. These two parameters indicate the extreme of possible failure surface boundaries by which the failure surface is surrounded. In other words, the maximum sum of the tensile force in the reinforcements will occur between these boundaries.

The angle pertaining to each part is obtained as $(\alpha_s - \alpha_{Lc})/n$. For the special case where α_{Lc} and α_s are equal, the multiplanar slip surface reverts to a planar shape in this technique. Consider θ_i as the angle respect to the vertical direction

$$\theta_i = (90 - \alpha_s) + \left(\frac{\alpha_s - \alpha_{Lc}}{n}\right) i \tag{10}$$

For $n=4$, as shown in Fig. 2, the sliding surface consists 4 segments begins from point C and ends at point A. When the soil wedge is divided to n layers, there are n reinforcement elements at distances equal to h_i elevated from the crest

$$h_i = \frac{i}{n} H \tag{11}$$

If X_i and Y_i represent the coordinates of an arbitrary point on

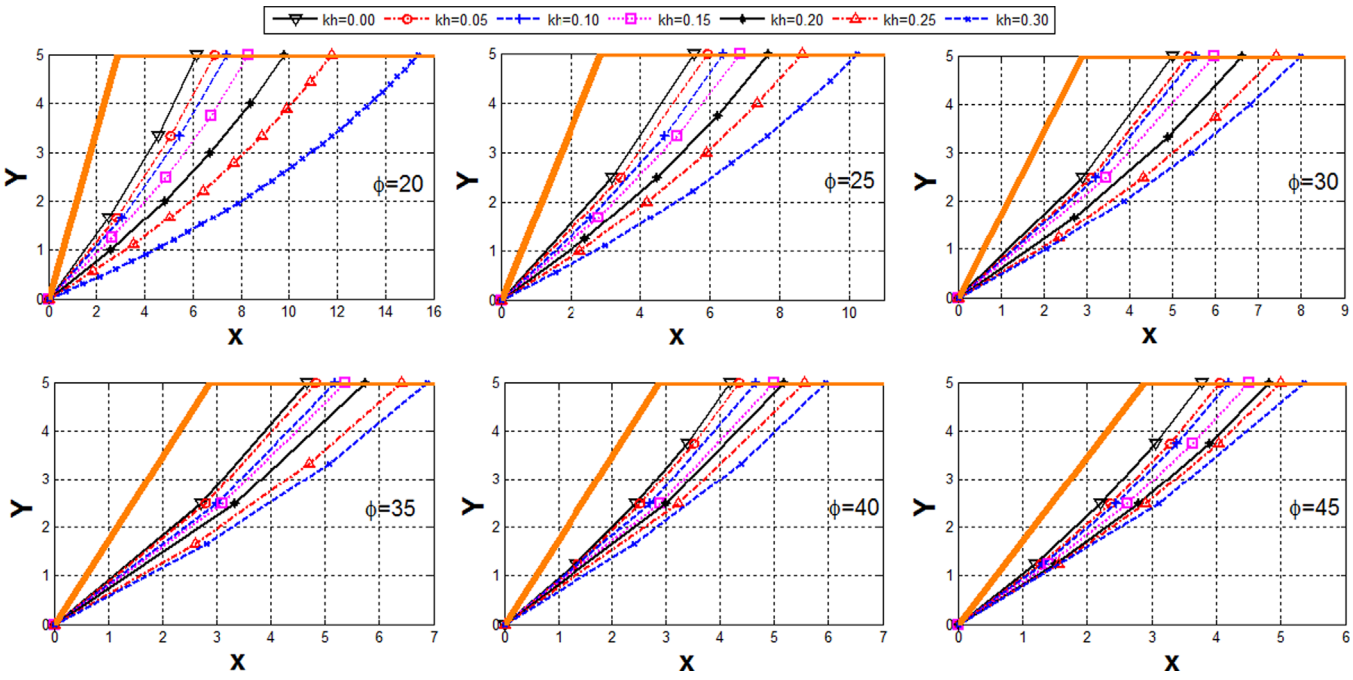

Fig. 7. Slip surface for different ϕ and $\beta = 45°$.

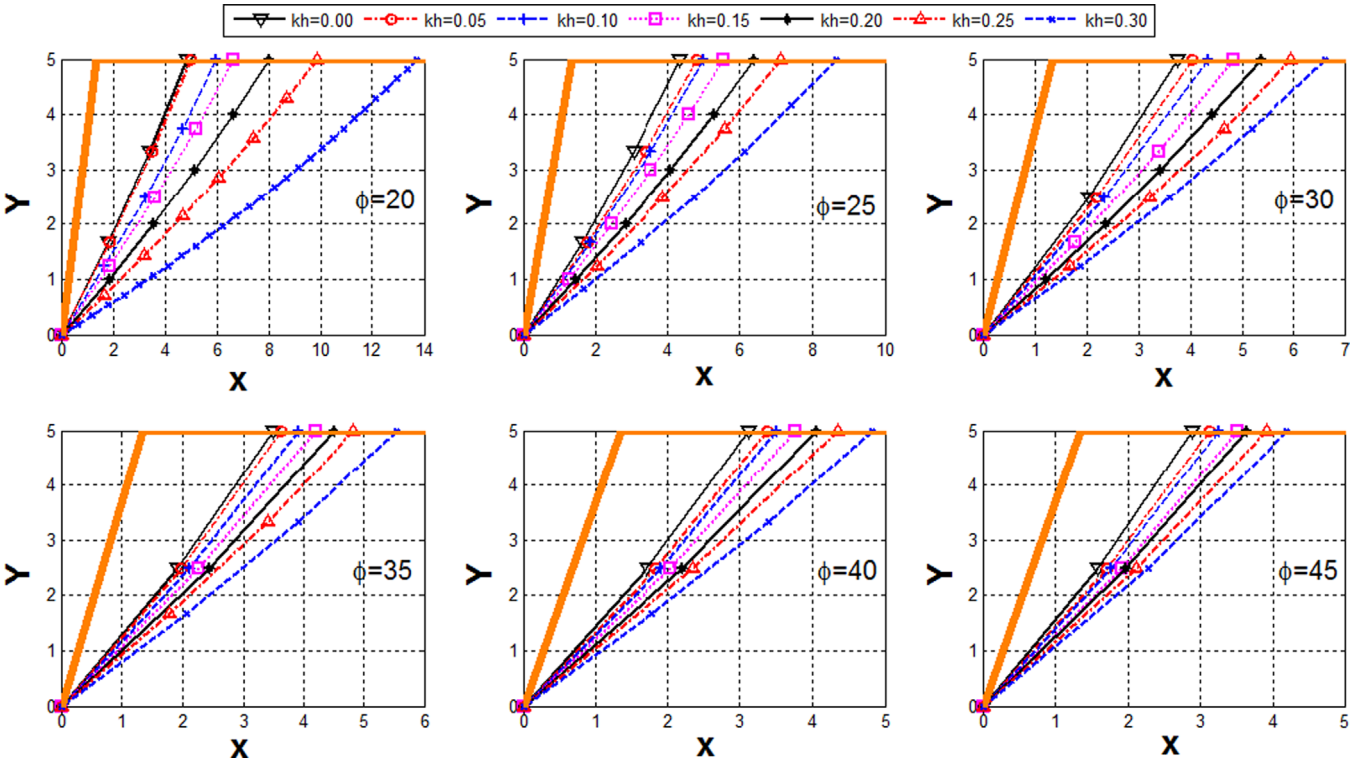

Fig. 8. Slip surface for different ϕ and $\beta = 60°$.

sliding surface, then

$$X_i = X_c - \frac{i}{n}H \times \tan(\theta_i)$$
$$Y_i = H - h_i = H - \frac{i}{n}H = H\left(\frac{n-i}{n}\right) \quad (12)$$

Now what remains for finding the slip configuration is a computerized algorithm to search in all possible configurations which have been suggested previously in this paper. MATLAB Program has been used for implementation of the procedure in this study. The flowchart of the procedure is shown in Fig. 3. Based on Fig. 3, it can be expressed that $\alpha_{Lc} \le \alpha_S \le 90$.

The effects of α_S for the case where $\gamma = 18$ and $k_h = 0.2$ are depicted in Fig. 4.

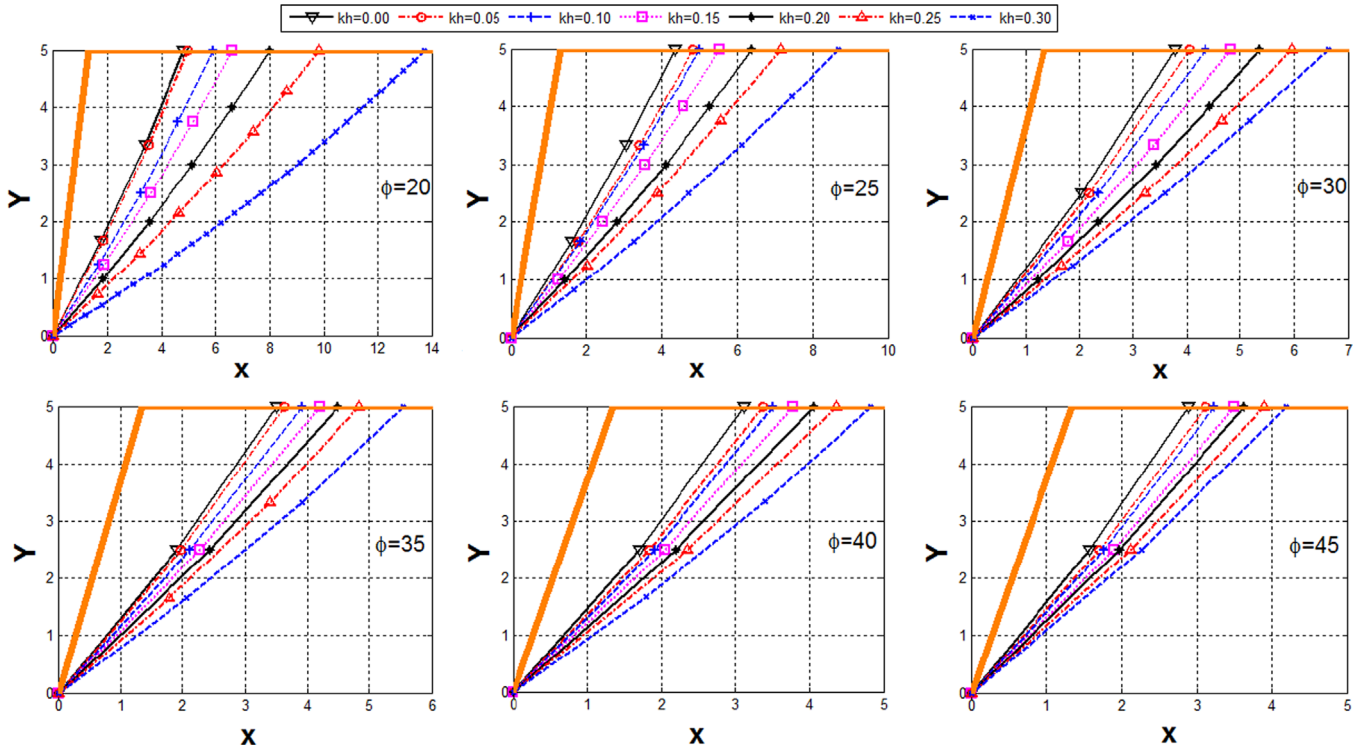

Fig. 9. Slip surface for different ϕ and $\beta = 75°$.

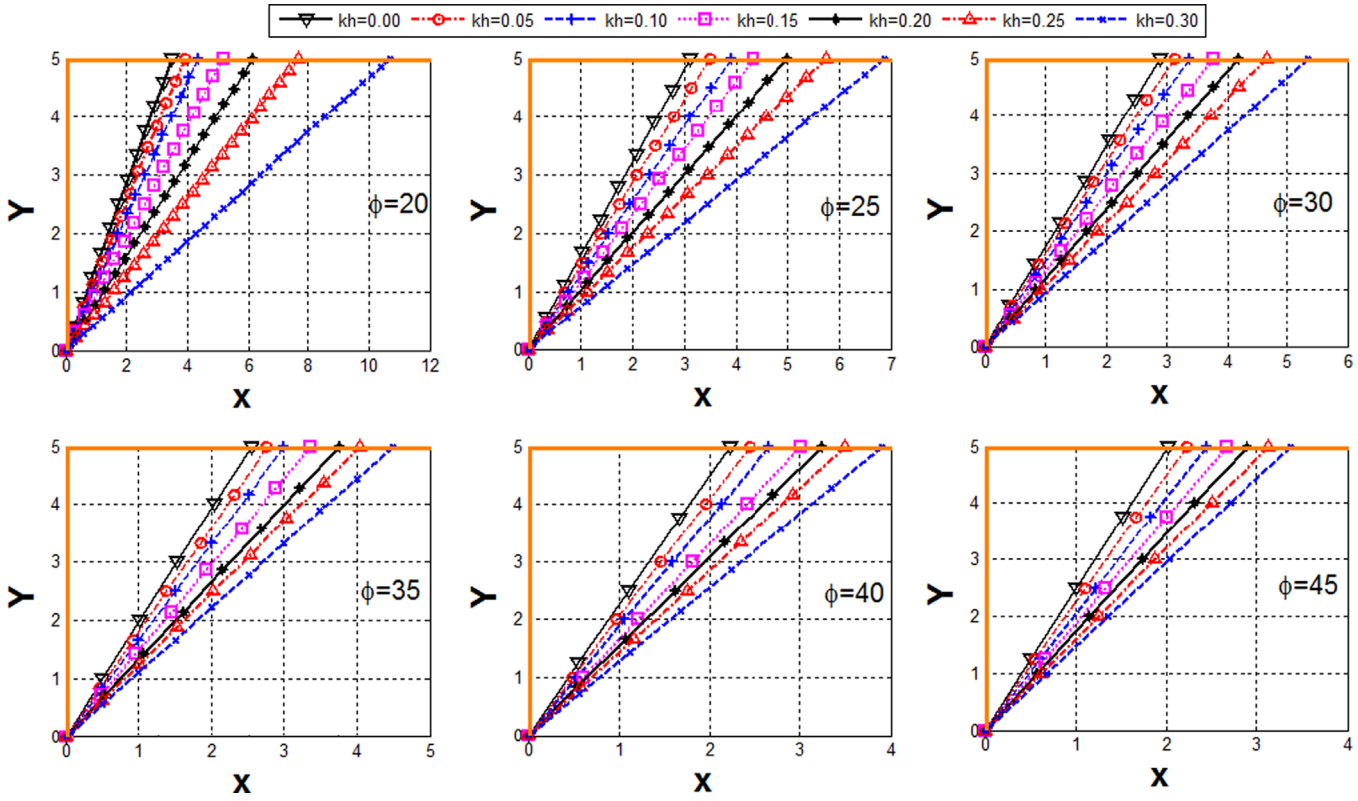

Fig. 10. Slip surface for different ϕ and $\beta = 90°$.

3. The generality of the method

Some of the more noticeable features of the proposed method can be summarized as:

- In the proposed method the number of horizontal slices is optimized in accordance with the flowchart shown in Fig. 3 in order to evaluate the maximum total reinforcement force, whereas the other methods use a predetermined number of slices.
- Force and moment equilibrium equations are considered simultaneously in each horizontal slice for the new model of

Table 7
Results of L_c/H for a slope with $\beta = 45°$ and $k_h = 0.2$ on optimized layers.

ϕ (deg)	L_c/H: ($\beta = 45, \gamma = 18$)					
	k_h=0.00		k_h=0.10		k_h=0.20	
	$n = 5$	n = optimum	$n = 5$	n = optimum	$n = 5$	n = optimum
20	0.70	0.60	0.90	0.90	1.35	1.35
25	0.55	0.40	0.70	0.60	0.90	0.90
30	0.40	0.30	0.55	0.40	0.70	0.70
35	0.25	0.15	0.40	0.30	0.50	0.50
40	0.20	0.10	0.30	0.20	0.40	0.30
45	0.15	0.05	0.20	0.10	0.30	0.20

Table 8
Results of L_c/H for a slope with $\beta = 75°$ and $k_h = 0.2$ on optimized layers.

ϕ (deg)	L_c/H: ($\beta = 75, \gamma = 18$)					
	k_h=0.00		k_h=0.10		k_h=0.20	
	$n = 5$	n = optimum	$n = 5$	n = optimum	$n = 5$	n = optimum
20	0.70	0.70	0.95	0.90	1.35	1.30
25	0.70	0.60	0.80	0.70	1.00	1.00
30	0.60	0.50	0.65	0.60	0.80	0.80
35	0.50	0.40	0.55	0.50	0.70	0.60
40	0.50	0.35	0.50	0.40	0.60	0.55
45	0.40	0.30	0.45	0.40	0.50	0.45

Table 9
Results of $(\sum_{i=1}^{n} T_i)_{max}$ (kN) for a slope with $k_h = 0.2$ on two kind of soil material slope in various slopes.

γ	β	$(\sum_{i=1}^{n} T_i)_{max}$ (kN)	
		$\varphi = 20$	$\varphi = 25$
18	**45**	**98.00**	**69.00**
	60	**112.00**	**85.00**
	75	**129.00**	**104.00**
	90	**151.00**	**127.00**
25	**45**	**136.12**	**95.43**
	60	**155.94**	**118.46**
	75	**178.65**	**143.75**
	90	**210.24**	**176.58**

Table 10
Safety factor of the optimum setup determined via the proposed method with classical Morgenstern–Price Limit Equilibrium Method.

β (deg)	ϕ (deg)	Safety factor				
		k_h=0.00	k_h=0.05	k_h=0.10	k_h=0.15	k_h=0.20
45	**25**	0.932	0.932	0.934	0.938	0.940
	30	0.994	0.978	0.969	0.972	0.976
	35	1.007	1.004	0.997	0.998	0.999
60	**25**	0.983	0.982	0.967	0.973	0.977
	30	1.013	1.014	1.009	1.008	1.002
	35	1.040	1.036	1.038	1.033	1.032
75	**25**	1.019	1.023	1.022	1.010	1.014
	30	1.051	1.048	1.043	1.034	1.021
	35	1.072	1.066	1.062	1.055	1.047

multiplanar sliding surface.

- Multiplanar slip surface used in this study (as well as Nimbalkar et al. [16]) furnishes more flexibility than pre-determined configurations such as log-spiral type used in many other methods.
- The main characteristics of the proposed method are presented in Table 1 alongside a number of similar methods in order to highlight the plausible differences.
- The presented configuration is independent of analysis method and therefore, the configuration presented can be used for vertical slice analytical methods, (e.g. Morgenstern–Price, Sarma and the other classical methods).
- In this approach, the extremes of possible failure surface boundaries can be determined by two angles of α_S and α_{LC}.
- Typically, in many design guidelines, a maximum spacing between reinforced elements is 1 m [31]. The optimization procedure can be used to optimize the vertical distance between reinforced layers in slope height.

4. Results and discussions

In order to illustrate the capability of proposed method for slope stability analysis, the procedure has been carried out for a homogeneous and cohesionless soil slope with height of 5 m. The geometrical (β and H), geotechnical (γ, c, ϕ) and design seismic coefficient (k_h) properties of the slope are given in Table 2. The soil wedge above the slip surface is subdivided into n horizontal slices parallel to reinforcement. The number of horizontal slices is optimized according to the flowchart in Fig. 3 in order to achieve the maximum of total reinforcement force. In this procedure, the slope inclination angle is assumed as 45–90° and the soil internal friction angle is changed from 20° to 45°.

The results of the stability analysis for the new model of multiplanar sliding surface are presented in Figs. 5 and 6 using the two dimensionless parameters of K and L_c/H. As shown in Fig. 2, L_c is the distance between the slip surface and the face of the slope on crest. It is noteworthy that L_c is equal to the maximum required reinforcement length.

As expected, the total normalized reinforcement force, K decreases with increase in internal friction angle, ϕ. Also, for slopes with larger inclination angle, β, the total reinforcing force, K, become higher. On the other hand, slopes with lower inclination angle and or soils with higher internal friction angle induced lower forces to reinforcements. These are shown in Fig. 5. Having the values of K, the maximum total reinforcement force, $(\sum_{i=1}^{n} T_i)_{max}$, in each case can be obtained from Eq. (9). This value for various slopes with different ϕ and k_h is evaluated and is given in Tables 3–6.

According to Eq. (9), both parameters K and $(\sum_{i=1}^{n} T_i)_{max}$ are linearly connected to each other. Therefore, similar results can be expressed for variation of L_c/H with respect to ϕ and k_h.

Fig. 6 presents the variation of L_c/H respect to ϕ for different values of k_h. As shown, values of L_c/H decrease monotonically as the internal friction angle increases. Also, values of L_c/H reduced slightly as the slope inclination angle increased. Higher coefficients of horizontal seismic acceleration, k_h requires longer L_c/H to maintain the slope stability.

In order to obtain the configuration of the slip surface, Eq. (12) can be used. The slip configurations obtained by the new model of multiplanar sliding surface for different β and ϕ are depicted in Figs. 7-10. According to these figures, for higher slope angles, the configurations of slip surfaces take planar shape. On the other hand, with increase in internal friction angle, the sliding wedge will become smaller. Thus, the maximum length of reinforcement required for the stability of the slope is reduced. The results also revealed that when the horizontal earthquake force increases, the sliding wedge would become wider.

In addition, the optimized results of the maximum required reinforcement length on two slope 45° and 75° are presented in Tables 7 and 8. Based on presented results in the Tables, the

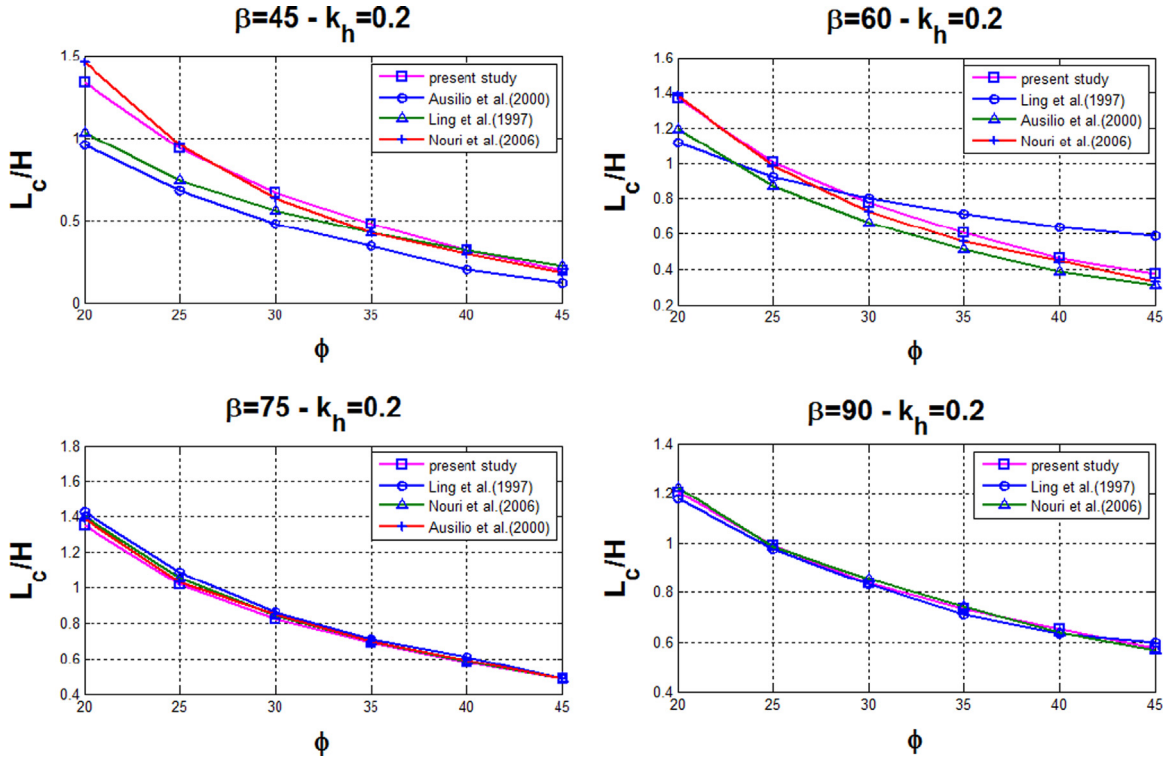

Fig. 11. L_c/H parameter with respect to ϕ ($\phi = 20 - 45$).

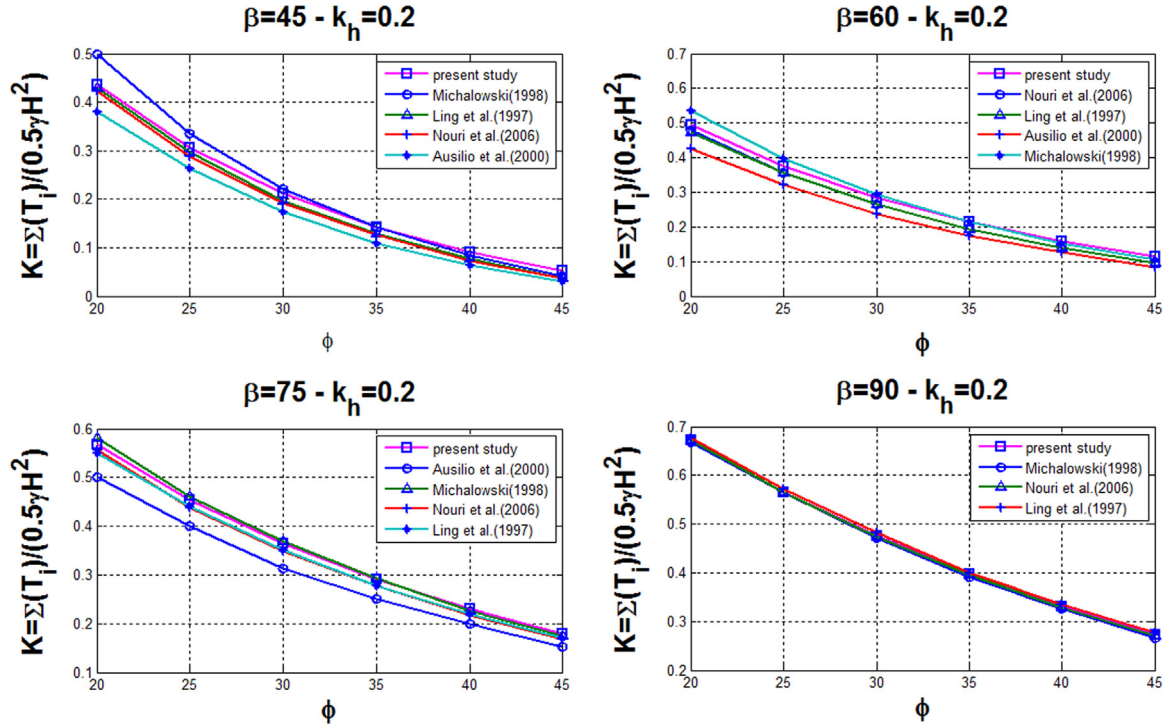

Fig. 12. K-parameter with respect to ϕ ($\phi = 20 - 45$).

maximum length of reinforcement required for the stability of the slope is sometime reduced until 30%. Then, the results of $(\sum_{i=1}^{n} T_i)_{\max}$ for $k_h = 0.2$ on the two soil materials with different specific weights $\gamma = 18$ and $\gamma = 25$ in various inclined slopes are compared in Table 9. As obtained in the table, values of $(\sum_{i=1}^{n} T_i)_{\max}$ increase monotonically as the unit weight of the soil.

5. Verification and comparison with previous studies

Before attempting to compare the results of the proposed procedure with other similar techniques, the ability of the proposed method to locate the critical slip surface is demonstrated by comparing the safety factor of the optimum setup determined via

Table 11
$(\sum_{i=1}^{n} T_i)_{max}$ (kN) obtained in different papers for a slope with $\beta = 90°$.

Papers	∅ (deg)	$(\sum_{i=1}^{n} T_i)_{max}$ (kN)			
		k_h=0.00	k_h=0.10	k_h=0.20	k_h=0.30
Leshchinsky [32]	**20**	*110*	*128*	*151*	*187*
	25	*95*	*110*	*126*	*153*
	30	*74*	*90*	*106*	*128*
Shahgholi et al. [9]	**20**	*110*	*128*	*151*	*187*
	25	*91*	*107*	*127*	*153*
	30	*75*	*89*	*106*	*128*
Choudhury et al. [33]	**20**	*110*	*130*	*157*	*202*
	25	*91*	*109*	*131*	*162*
	30	*75*	*91*	*110*	*135*
Present study	**20**	*111*	*128*	*151*	*187*
	25	*92*	*108*	*127*	*153*
	30	*76*	*90*	*107*	*128*

the proposed method with classical Morgenstern–Price Limit Equilibrium Method. The results are presented in Table 10, where it can be noted that a reduction of 3–7% in factor of safety is achieved by the proposed method, signifying the relative correctness of the method as well as an advancement of the solution procedure.

Furthermore, the performance of the proposed method is examined in comparison with a number of other methods (e.g. Ling et al. [4], Michalowski [6], Ausilio et al. [7] and Nouri et al. [10], Ling and Leshchinsky [5], Shahgholi et al. [9], Choudhury et al. [33]). The slip surface configuration was pre-assumed in most of the previous studies. The significance of the method proposed in this study is to yield the slip configuration.

The results considered in Figs. 11 and 12 are related to new multiplanar sliding surface. Then, the maximum sum of the tensile force in the reinforcements is compared with a number of other methods in Table 11.

As shown in Figs. 11 and 12, the results of this study are between the extreme values reported by other papers. The results for the case where $\beta = 90°$ and $k_h = 0.2$ are approximately the same. Also, values of L_c/H reduced slightly as the slope inclination angle increased. Higher coefficients of horizontal seismic acceleration, k_h, requires longer L_c/H to maintain the slope stability.

Based on presented results in Table 11, the maximum sum of the tensile force in the reinforcements for the case where $\beta = 90°$ are approximately the same with others and it can be noted that there is a difference of 1.5–7.5% with Choudhury et al. [33] method.

5.1. Recommendations for future work

The current study can be extended further to work the following:

1. Evaluation of other failure conditions including failure under surcharge.
2. Reinforced slopes stability analysis using together pseudo-dynamic approach and present configuration.
3. Employing new multiplanar configuration for vertical slice analytical methods.
4. Considering current procedure for different inclination angles of reinforcement.
5. Employing the approach for non-uniform slopes or for pore pressures existence.

6. Conclusions

The objective of this paper is to determine the probable multiplanar slip surface in the seismic stability analysis of reinforced 2D slopes using Horizontal Slice Method and pseudo-static approach. The procedure is capable to obtain the maximum total reinforcement force using the comprehensive formulation of horizontal slices. The following results were obtained eventually:

1) Maximum sum of the tension force in the reinforcement indicates that the employed slip surface is critical.
2) With increase in horizontal seismic acceleration, the reinforcements force increases.
3) With increase in slope angle, the failure surface changes from curved surface to planar shape.
4) With increase of the internal friction angle ϕ, the slip plane nears the slope face.
5) The results of the analysis show that the value of K is almost less than 1 and decreases with increase in ϕ while β is constant. Also, the value of K increases with increase in β while ϕ remains constant.
6) With increase of the specific weight γ, values of $(\sum_{i=1}^{n} T_i)_{max}$ increase.
7) With optimizing the layers, values of L_c/H decrease.

Acknowledgment

The authors wish to thank supports provided by Faculty of Civil Engineering in Babol Noshirvani University of Technology and also Faculty of Civil Engineering in K.N. Toosi University of Technology.

References

[1] Richardson Gregory N, Lee Kenneth L. Seismic design of reinforced earth walls. J Geotech Eng Div 1975;101(2):167–88.
[2] Bathurst RJ, Cai Z. Pseudo-static seismic analysis of geosynthetic reinforced segmental retaining walls. Geosynth Int 1995;2(5):787–830.
[3] Jones CJFP, Clarke D. The residual strength of geosynthetic reinforcement subjected to accelerated creep testing and simulated seismic events. Geotext Geomembr 2007;25(3):155–69.
[4] Ling HI, Leshchinsky D, Perry EB. Seismic design and performance of geosynthetic-reinforced soil structures. Geotechnique 1997;47(5):933–52.
[5] Ling HI, Leshchinsky D. Effects of vertical acceleration on seismic design of geosynthetic-reinforced soil structures. Geotechnique 1998;48(3):347–73.
[6] Michalowski Radoslaw L. Soil reinforcement for seismic design of geotechnical structures. Comput Geotech 1998;23(1):1–17.
[7] Ausilio E, Conte E, Dente G. Seismic stability analysis of reinforced slopes. Soil Dyn Earthq Eng 2000;19(3):159–72.
[8] Lo SCR, Xu DW. A strain-based design method for the collapse limit state of reinforced soil walls or slopes. Can Geotech J 1992;29(5):832–42.
[9] Shahgholi M, Fakher A, Jones CJFP. Horizontal slice method of analysis. Geotechnique 2001;51(10):881–6.
[10] Nouri H, Fakher A, Jones CJFP. Development of horizontal slice method for seismic stability analysis of reinforced slopes and walls. Geotext Geomembr 2006;24(3):175–87.
[11] Saran Swami, Garg KG, Bhandari RK. Retaining wall with reinforced cohesionless backfill. Journal Geotech Eng 1992;118(12):1869–88.
[12] Narasimha Reddy GV, Madhav MR, Saibaba Reddy E. Pseudo-static seismic analysis of reinforced soil wall—effect of oblique displacement. Geotext Geomembr 2008;26(5):393–403.
[13] Sengupta Aniruddha, Upadhyay Anup. Locating the critical failure surface in a slope stability analysis by genetic algorithm. Appl Soft Comput 2009;9(1):387–92.
[14] Kalatehjari R, Ali N, Kholghifard M, Hajihassani M. The effects of method of generating circular slip surfaces on determining the critical slip surface by particle swarm optimization. Arab J Geosci 2014;7(4):1529–39.
[15] Zolfaghari Ali R, Heath Andrew C, McCombie Paul F. Simple genetic algorithm search for critical non-circular failure surface in slope stability analysis. Comput Geotech 2005;32(3):139–52.
[16] Nimbalkar Sanjay S, Choudhury Deepankar, Mandal JN. Seismic stability of reinforced-soil wall by pseudo-dynamic method. Geosynth Int 2006;13(3):111–9.
[17] Leshchinsky Dov, Lambert Greg. Failure of cohesionless model slopes reinforced with flexible and extensible inclusions. Transp Res Rec 1991;1330.
[18] Sil Arjun, Dey Ashim Kanti. Dynamic performance of cohesive slope under

seismic loading. Int J Civ Struct Eng 2014;5(1):1–14.
[19] Morgenstern NR, Eo Price V. The analysis of the stability of general slip surfaces. Geotechnique 1965;15(1):79–93.
[20] Spencer Eric. Thrust line criterion in embankment stability analysis. Geotechnique 1973;23(1).
[21] Geo-Slope International Ltd. Geo-slope manual. Calgary, Alberta, Canada; 2004.
[22] Prater Edward G. Yield acceleration for seismic stability of slopes. J Geotech Eng Div 1979;105(5):682–7.
[23] Spencer E. A method of analysis of the stability of embankments assuming parallel inter-slice forces. Geotechnique 1967;17(1):11–26.
[24] Hu Cong, Jimenez Rafael, Li Shu-cai, Li Li-ping. Determination of critical slip surfaces using mutative scale chaos optimization. J Comput Civil Eng 2013.
[25] Nguyen Van Uu. Determination of critical slope failure surfaces. J Geotech Eng 1985;111(2):238–50.
[26] Malkawi Abdallah I Husein, Hassan Waleed F, Sarma Sarada K. Global search method for locating general slip surface using Monte Carlo techniques. J Geotech Geoenviron Eng 2001;127(8):688–98.
[27] Goh Anthony TC. Genetic algorithm search for critical slip surface in multiple-wedge stability analysis. Can Geotech J 1999;36(2):382–91.
[28] Sarma SK, Tan D. Determination of critical slip surface in slope analysis. Géotechnique 2006;56(8):539–50.
[29] Stamatopoulos Constantine A, Mavromihalis Constantine, Sarma Sarada. Correction for geometry changes during motion of sliding-block seismic displacement. J Geotech Geoenviron Eng 2011;137(10):926–38.
[30] Sarma SK. Stability analysis of embankments and slopes. J Geotech Eng 1979;105(12):1511–24.
[31] Nouri H, Fakher A, Jones CJFP. Evaluating the effects of the magnitude and amplification of pseudo-static acceleration on reinforced soil slopes and walls using the limit equilibrium horizontal slices method. Geotext Geomembr 2008;26(3):263–78.
[32] Leshchinsky D, ReSlope. Geotechnical fabric report 15 (1). Industrial Fabrics Association International; 1997. p. 40–6.
[33] Choudhury Deepankar, Modi Deepa. Displacement-based seismic stability analyses of reinforced and unreinforced slopes using planar failure surfaces. GeoCongress. Geotechnical special publication no. 181; 2008. p. 1–10.